

Design by Monte Carlo method of a thermal neutron device using a $^{241}\text{Am}/^9\text{Be}$ source and high-density polyethylene moderator

Cevallos-Robalino, L. E., García-Fernández, G. F., Lorente, A., Gallego, E., Vega-Carrillo, H. R., & Guzmán-García, K. A.

► To cite this version:

Cevallos-Robalino, L. E., García-Fernández, G. F., Lorente, A., Gallego, E., Vega-Carrillo, H. R., & Guzmán-García, K. A. (2019). Design by Monte Carlo method of a thermal neutron device using a $^{241}\text{Am}/^9\text{Be}$ source and high-density polyethylene moderator. *Applied Radiation and Isotopes*, 151, 150–156.
doi:10.1016/j.apradiso.2019.05.040

Published version.

Published September 2019

Archivo Digital UPM houses in digital format the academic and scientific documentation (theses, pfc, articles, etc.) generated at the institution and makes it accessible through the Internet, within the framework of the Budapest Open Access Initiative and the Berlin Declaration, of which the Universidad Politécnica de Madrid is a signatory.

El **Archivo Digital UPM** alberga en formato digital la documentación académica y científica (tesis, pfc, artículos, etc.) generada en la institución, y la hace accesible a través de Internet, en el marco de la Iniciativa por el Acceso Abierto de Budapest y la Declaración de Berlín, de la que es signataria la Universidad Politécnica de Madrid.

Design by Monte Carlo method of a thermal neutron device using a $^{241}\text{Am}/^9\text{Be}$ source and high-density polyethylene moderator

Lenin E. Cevallos-Robalino^{a,b,*}, Gonzalo F. García-Fernández^a, Alfredo Lorente^a, Eduardo Gallego^a, Hector Rene Vega-Carrillo^c, Karen A. Guzmán-García^a

^a Departamento de Ingeniería Energética, ETSI Industriales, Universidad Politécnica de Madrid, José Gutiérrez Abascal 2, 28006, Madrid, Spain

^b Grupo de Investigación en Sistemas de Control y Robótica, GISCOR, Universidad Politécnica Salesiana, C. Robles 107 Chambers, 090108, Guayas, Guayaquil, Ecuador

^c Unidad Académica de Estudios Nucleares, Universidad Autónoma de Zacatecas, C. Ciprés No. 10, Fracc. La Peñuela, 981000, Zacatecas, Zac, Mexico

HIGHLIGHTS

- A device has been designed to increase thermal neutron flux from a $^{241}\text{Am}/^9\text{Be}$ source, through the neutron moderation.
- The system can be used to identify trace materials by Neutron Activation Analysis.
- Three different alternative moderator materials, water, graphite and high-density polyethylene (HDPE), were simulated.
- The system performance was evaluated with the MCNP6 code.

ARTICLE INFO

Keywords:

MCNP6 code

$^{241}\text{Am}/^9\text{Be}$ source

Dosimetry equipment

ABSTRACT

A thermal neutron system intended to be used in neutron activation analysis has been designed by Monte Carlo methods. The device is based on a $^{241}\text{Am}/^9\text{Be}$ neutron source of 111 GBq, placed inside a cylindrical cavity open inside a parallelepiped of moderator material. Three different moderator materials, water, graphite and high-density polyethylene (HDPE), were simulated to check what is the most suitable for the detection system, concluding that HDPE reach the better performance. The device achieves an increased thermal neutron flux by taking advantage of neutron moderation in the polyethylene and the neutron scattering in the irradiation chamber walls. The thermal fluence rates obtained were $904\text{ cm}^{-2}\text{ s}^{-1}$, i.e. $8.144\text{ cm}^{-2}\text{ s}^{-1}\text{ GBq}^{-1}$, with a fraction of thermal neutrons at the best point of 83% of pristine fast neutrons emitted by the source. The device has been designed by Monte Carlo techniques using the MCNP6 code, and the main tasks developed were to select the moderator material and to maximize the thermal neutrons flux in the irradiation chamber.

1. Introduction

Neutrons and gamma rays are able to penetrate high density objects and identify hidden materials in bulk detection (Csikai and Dóczy, 2007). Since the discovery of neutrons, scattering techniques using these particles were applied to study different physical phenomena. Taking advantage of the fact that neutrons have no charge and their interactions with electrons are weak, they can penetrate inside bulks, activate their atoms and allow to identify chemical composition of materials by studying the gamma rays emitted. (Belushkin, 1999). Among techniques that use neutrons to detect threats, Neutron Activation Analysis (NAA) is a very useful and sensitive analytical procedure for performing both qualitative and quantitative multielemental analysis of components in a variety of samples (Hamidatou et al.,

2013). Neutron interaction techniques are useful in estimating the major constituent elements in explosives and narcotics, such as hydrogen (H), oxygen (O), carbon (C) and nitrogen (N) (Hassan, 2009), allowing to determine the exact concentration of a suspect chemical element by studying both the energy and the intensity of the gamma radiation emitted (Elsheikh et al., 2012). The key factor for an optimal performance in neutron activation is to have a thermal neutron fluence rate of about $10^3\text{ cm}^{-2}\text{ s}^{-1}$ at the location of the analysed sample (Bedogni et al., 2017).

The NAA is an elemental method to characterize materials founded in the measure of indirect parameters. The detection process begin when neutrons interact with nuclei producing the activation of several atoms, which return to their ground state emitting characteristic gamma radiation of the excited state of each activated chemical

* Corresponding author. Universidad Politécnica de Madrid, C. José Gutiérrez Abascal, 2, 28006, Madrid, Spain.

E-mail address: lcevallos@ups.edu.ec (L.E. Cevallos-Robalino).

element (Douglas Reilly et al., 1991). The activation induced by neutrons directly depends on the nuclei cross sections and the irradiation time (Vega Carrillo et al., 2016).

The excited nuclei emit a prompt gamma radiation (10^{-14} s), with a characteristic energy, usually between 2 and 10 MeV, depending on the chemical element and its excited electronic level. The nuclear reaction, (n, γ) , is known as neutron capture with gamma emission (Hee Jung and Song, 2009), and to get the energy spectrum a scintillator detector and gamma spectrometry is commonly used (Travesi, 1975). This analytical technique is usually known as Prompt Gamma NAA (PGNAA).

Isotopic neutron sources of (α, n) type, as $^{241}\text{Am}/^9\text{Be}$ employed in this work, have found many applications, especially in scientific research and in calibration field. The ^{241}Am isotope is a strong α particle emitter and mixed with Beryllium produces neutrons through the $^9\text{Be}(\alpha, n)^{12}\text{C}$ reaction (Vitorelli et al., 2005). The neutron spectrum emitted by a $^{241}\text{Am}/^9\text{Be}$ source lie down between 0.8 and 10 MeV, with a mean energy of 3.2 MeV (Vega Carrillo and Martinez Ovalle, 2016).

The interaction of neutrons with matter causes ionization in the environment through a complicated mechanism involving the emission of energetic secondary charged particles (Chilton et al., 1984). Thus, different concrete types or polymer composites are employed as neutron shielding materials (Gallego et al., 2009) (El Sayed Abdo et al., 2003) (Vega Carrillo et al., 2007). Furthermore, neutron moderating and reflecting materials are required to obtain a suitable level of flux at the irradiation chamber, (Bedogni et al., 2016). Between the alternative materials, high density polyethylene (HDPE), alone or combined with another materials, is an effective neutron shielding and shows an excellent attenuation behavior without meaningful reducing the neutron flux (Yasin and Khan, 2008).

Although high intensity sources are employed in detection systems of suspect materials, the energetic fast neutrons released from the source need to be moderated to improve their interactions with atoms in the bulk, since the absorption cross section of fast neutrons is much smaller than scattering cross section of thermal neutrons (Gokhale and Hussein, 1997). Neutrons lose energy by scattering with atoms and become thermal after a number of collisions. The thermalization process takes many fewer collisions when scattering with hydrogen as compared to other elements (Bom et al., 2008).

Another material frequently used to build moderating assemblies with polyethylene is graphite. Although graphite produces fewer gamma radiation than polyethylene it requires thicker layers compared to HDPE because graphite has lower scattering cross section and less average energy loss per collision (Lacoste et al., 2004; Glasstone and Sesonske, 1968). Thus, usually polyethylene is suggested due to its better moderating performance (Lee et al., 2012), that allows to reach high thermal neutron fluence rates using either isotopic sources or neutron generators (Datema et al., 2002).

The gamma rays background with an energy of 2.223 MeV (Turhan et al., 2004) is mainly coming from the $^1\text{H}(n, \gamma)^2\text{H}$ reaction (with a cross section $\sigma_{\text{th}} = 0.3327 \pm 0.007$ b for thermal neutrons) in hydrogenous materials of moderators (Soppera et al., 2014).

As a summary, Table 1 displays properties of several elements as neutron moderators (Glasstone and Sesonske, 1968; Soppera et al., 2014).

The objective of this work was to design a moderator assembly producing the maximum thermal neutron flux from a $^{241}\text{Am}/^9\text{Be}$ isotopic neutron source. Thermal neutrons will be used to identify and characterize materials by PGNAA.

2. Materials and methods

The device is inspired in the developments by (Bedogni et al., 2016) and (Bedogni et al., 2017). It is based on a $^{241}\text{Am}/^9\text{Be}$ source placed inside a moderator block with an empty cylindrical chamber inside. All the simulations were made with the Monte Carlo code MCNP6 (Pelowitz et al., 2014).

Table 1

Properties of materials commonly used as neutron moderators (based on (Glasstone & Sesonske, 1968; Soppera et al., 2014)).

Element	Mass Number	Collisions needed to reach thermal energy level	Cross-section scattering σ_s (barn)	Cross-section absorption σ_a (barn)
Hydrogen	1	18	30.08 ± 0.25	0.3327 ± 0.007
Deuterium	2	25	4.24 ± 0.06	0.00051 ± 0.00002
Helium	4	43	0.8635 ± 0.01	–
Beryllium	9	86	6.4983 ± 0.04	0.0100 ± 0.0005
Graphite	12	114	4.9478 ± 0.05	0.003862 ± 0.0001
Uranium	238	2172	9.2397 ± 0.05	2.6832 ± 0.03

Externally, the system is a parallelepiped box with dimensions $90 \text{ cm} \times 70 \text{ cm} \times 76 \text{ cm}$. Internally, it has a cylindrical irradiation chamber inside with dimensions, 70 cm long \times 31 cm diameter. The $^{241}\text{Am}/^9\text{Be}$ neutron source is housed in the chamber, with a shadow cylinder placed between the irradiation area and the source, to take advantage of backscattering neutrons. The system has a third hole, independent of the previous ones, where it would be possible to house a second neutron source.

The $^{241}\text{Am}/^9\text{Be}$ neutron source considered is from the Neutron Measurements Laboratory of the Energy Engineering Department of Universidad Politécnic de Madrid (LMN UPM). It has 111 GBq nominal activity, with a neutron emission rate of $(5.83 \pm 0.14) \cdot 10^6 \text{ s}^{-1}$ (Vega Carrillo et al., 2009). Its real dimensions and capsule details and material have been taken into account in the MCNP6 model.

The MCNP6 model of the system with details is shown in Fig. 1.

Several simulations using MCNP6 code were carried out to select the appropriate moderator material between HDPE, graphite or water and a suitable geometry of the system with the goal to maximize the thermal fluence rate of neutrons coming from the $^{241}\text{Am}/^9\text{Be}$ source.

Neutron fluence rates inside and outside the irradiation chamber were calculated using F5 tallies, considering 222 energy groups of the neutron spectra. The simulated number of histories was 10^8 to reach calculations uncertainties smaller than 5% in the calculations. The neutron cross section data library used was ENDF/B VII, for neutrons with $E < 20 \text{ MeV}$. The transport of thermal neutron, $E < 1 \text{ eV}$, in polyethylene was considered through $S(\alpha, \beta)$ treatment (Pelowitz et al., 2014).

The total fluence rate obtained from the Monte Carlo calculated spectra was multiplied by the source strength. Neutron spectra were calculated at several positions, to study the points at which the thermal flux would be higher. Also, MCNP6 DE and DF tally cards were used to convert particle flux to dose equivalent rate. The operational quantity ambient dose equivalent, $H^*(10)$, was calculated with the expression (1):

$$\dot{H}^*(10) = \int_{E_i}^{E_f} \dot{\Phi}_E(E) h^*(10, E) dE \quad (1)$$

Where $\dot{\Phi}_E$ is the fluence rate as a function of energy for a given neutron field, obtained from MCNP6, and $h^*(10, E)$ is the fluence to ambient dose equivalent conversion function, whose values are indicated in (ICRP, 1996), as a function of the neutron energy. The ambient dose equivalent rate, $\dot{H}^*(10)$ was calculated at six points outside the system indicated in Fig. 2, whilst Fig. 3 show the points where neutron fluxes and spectra were calculated inside the chamber.

3. Results

The calculated ambient dose equivalent rate from both neutron and gamma contributions, at the points out of the assembly are displayed in Table 2. Points 1, 2, 3 and 4 are in contact with the surface of the

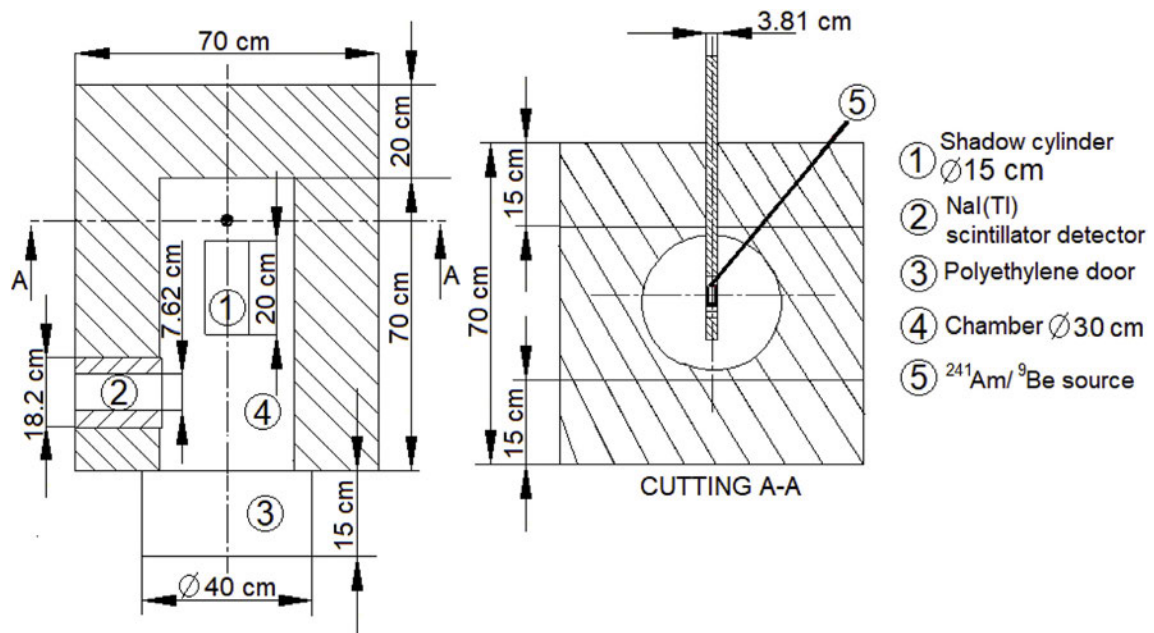


Fig. 1. MCNP6 model of the assembly showing dimensions. Sectional views at planes (X;Y;0) and (0;Y;Z).

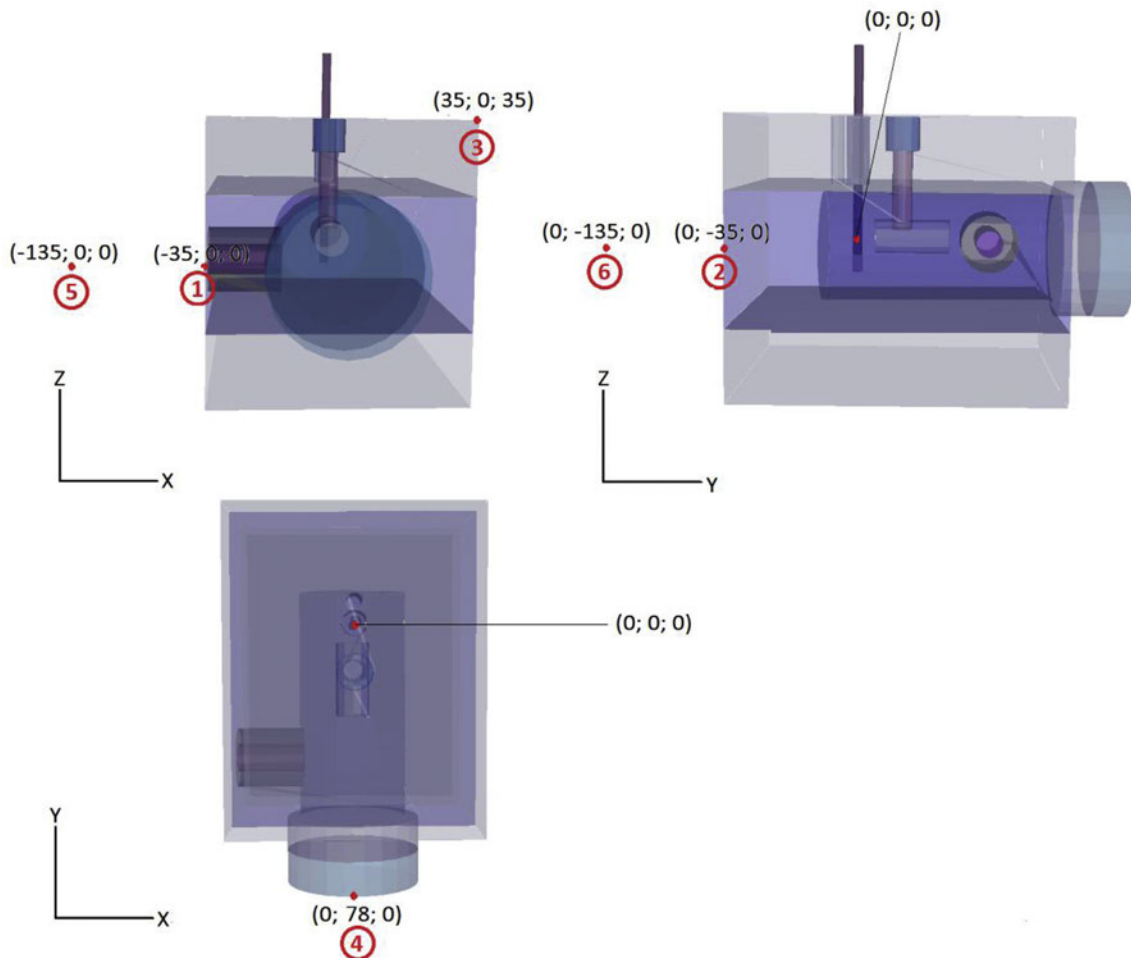


Fig. 2. Points used in the calculation of $\dot{H}^*(10)$, outside the chamber, in coordinate axes, X, Y, Z.

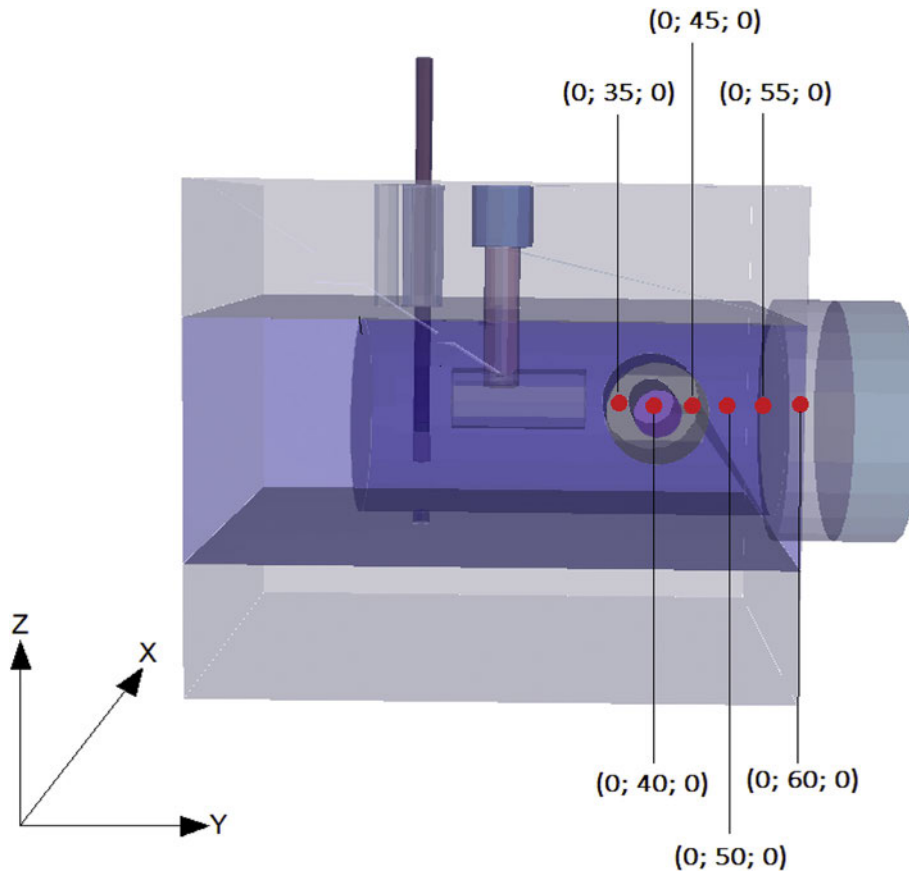


Fig. 3. Points used in the calculation, inside the chamber, in coordinate axes, X, Y, Z.

assembly, while points 5 and 6 are those giving the higher dose at 1 m distance from the surface of the moderator. Results for the three moderators, water, graphite and HDPE are compared. As it can be seen, while photon contribution to dose is higher in water and HDPE, HDPE provides the smaller total doses. The total ambient dose equivalent rate distribution around the HDPE assembly – sectional view by the (X;0;Z) plane cutting the source – is represented in Fig. 4.

Fig. 5 displays the lethargy spectra of neutron fluence depending on the distance to the source, from 35 cm to 50 cm inside the device chamber, at the points indicated in Fig. 3, for the three moderator materials, water, graphite and HDPE. The resulting thermal neutron flux ($E < 0.4$ eV) at each point is also indicated. The theoretical optimal configuration is with graphite at distances 35 cm and 40 cm from the $^{241}\text{Am}/^9\text{Be}$ source. Nevertheless, graphite makes necessary to use thicker layers compared to HDPE because of its lower scattering cross section and smaller average energy loss per collision (Lacoste et al., 2004).

The calculated neutron fluence rate per energy intervals values at point (0; 40; 0) at 40 cm from source are shown in Table 3, for the three

moderator materials. Using HDPE, the resulting thermal neutron flux ($E < 0.4$ eV) is $(9.04\text{E}+02 \pm 0.9 \text{ cm}^{-2}\text{s}^{-1})$. Results summarized in Table 3 show higher values of flux corresponding to graphite and comparable between water and HDPE moderators.

Fig. 6 shows the calculated thermal neutron ($E < 0.4$ eV) fluence rate along vertical radius points ($Z = 6; 8; 10; 12$ and 14 cm) at $X = 0$ and $Y = 40; 45; 50; 55$ cm from the source, with HDPE moderator. As it can be observed, the best results are obtained always for a distance of 40 cm between the source and the irradiation plane. However, at 55 cm the obtained flux is almost uniform in a wide spatial region.

Finally, Fig. 7 shows the energy distribution of neutron fluence along the main plane of irradiation, considering six different distances from the source, and HDPE as moderator.

4. Discussion and conclusions

As it was shown in Table 2, the ambient dose equivalent rate around the system depends upon the moderator, with water and HDPE offering similar values. Although graphite could give a slightly higher thermal

Table 2
Calculated ambient dose equivalent rate at points in contact and at 1m out of the assembly.

No.	Water			Graphite			HDPE		
	$\dot{H}^*(10)$ $\mu\text{Sv/h}$ - neutrons	$\dot{H}^*(10)$ $\mu\text{Sv/h}$ - photons	$\dot{H}^*(10)$ Total $\mu\text{Sv/h}$	$\dot{H}^*(10)$ $\mu\text{Sv/h}$ - neutrons	$\dot{H}^*(10)$ $\mu\text{Sv/h}$ - photons	$\dot{H}^*(10)$ Total $\mu\text{Sv/h}$	$\dot{H}^*(10)$ $\mu\text{Sv/h}$ - neutrons	$\dot{H}^*(10)$ $\mu\text{Sv/h}$ - photons	$\dot{H}^*(10)$ Total $\mu\text{Sv/h}$
1	1.26E+02	5.03E+02	6.30E+02	6.54E+02	4.98E+02	1.15E+03	7.48E+01	5.08E+02	5.82E+02
2	9.49E+01	4.68E+02	5.62E+02	5.71E+02	4.59E+02	1.03E+03	5.40E+01	4.70E+02	5.24E+02
3	1.03E+01	1.49E+02	1.60E+02	1.05E+02	1.46E+02	2.51E+02	4.01E+00	1.52E+02	1.56E+02
4	1.88E+00	3.95E+01	4.14E+01	3.61E+01	3.83E+01	7.45E+01	4.39E-01	4.00E+01	4.04E+01
5	6.32E+00	3.23E+01	3.86E+01	3.53E+01	3.17E+01	6.70E+01	3.10E+00	3.18E+01	3.49E+01
6	5.65E+00	3.15E+01	3.72E+01	3.41E+01	3.09E+01	6.50E+01	7.48E+01	5.08E+02	5.82E+02

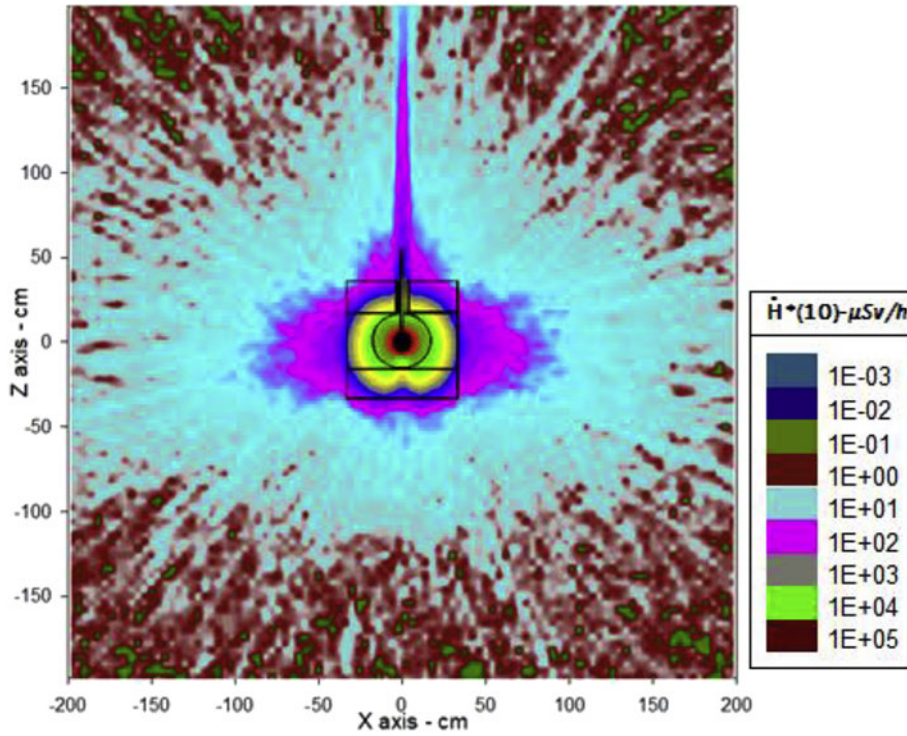


Fig. 4. Total ambient dose equivalent distribution around the HDPE assembly; sectional view by the (X;0;Z) plane.

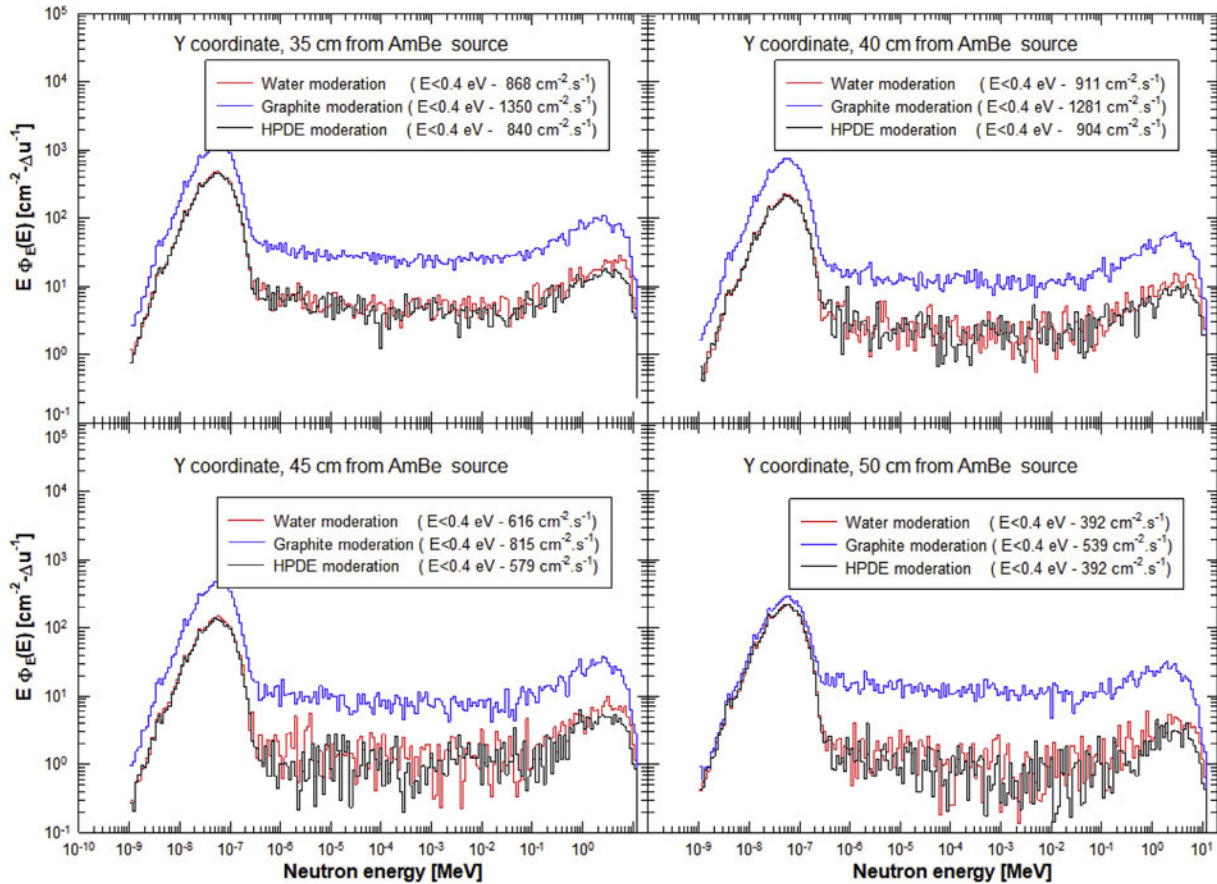


Fig. 5. Neutron fluence spectra at points inside the irradiation chamber with indication of the thermal flux obtained ($E < 0.4 \text{ eV}$).

Table 3

Calculated neutron flux per energy intervals at the point (0; 40; 0), for the three moderator materials.

Water			Graphite			HDPE		
Energy	cm ² s ⁻¹	Uncertainty ±	Energy	cm ² s ⁻¹	Uncertainty ±	Energy	cm ² s ⁻¹	Uncertainty ±
2.50E-08	2.29E+02	2.29E-01	2.50E-08	3.08E+02	3.08E-01	2.50E-08	2.27E+02	2.27E-01
4.00E-07	6.82E+02	6.82E-01	4.00E-07	9.73E+02	8.76E-01	4.00E-07	6.77E+02	6.77E-01
1.00E-06	8.32E+00	1.91E-02	1.00E-06	3.50E+01	4.20E-02	1.00E-06	8.91E+00	2.05E-02
1.00E-05	1.73E+01	3.45E-02	1.00E-05	7.80E+01	7.80E-02	1.00E-05	1.85E+01	3.52E-02
1.00E-03	2.92E+01	5.54E-02	1.00E-03	1.51E+02	1.36E-01	1.00E-03	3.14E+01	5.66E-02
1.00E+00	4.97E+01	1.04E-01	1.00E+00	2.92E+02	2.63E-01	1.00E+00	5.54E+01	1.11E-01
3.00E+00	1.80E+01	1.80E-02	3.00E+00	1.08E+02	1.62E-01	3.00E+00	2.10E+01	6.93E-02

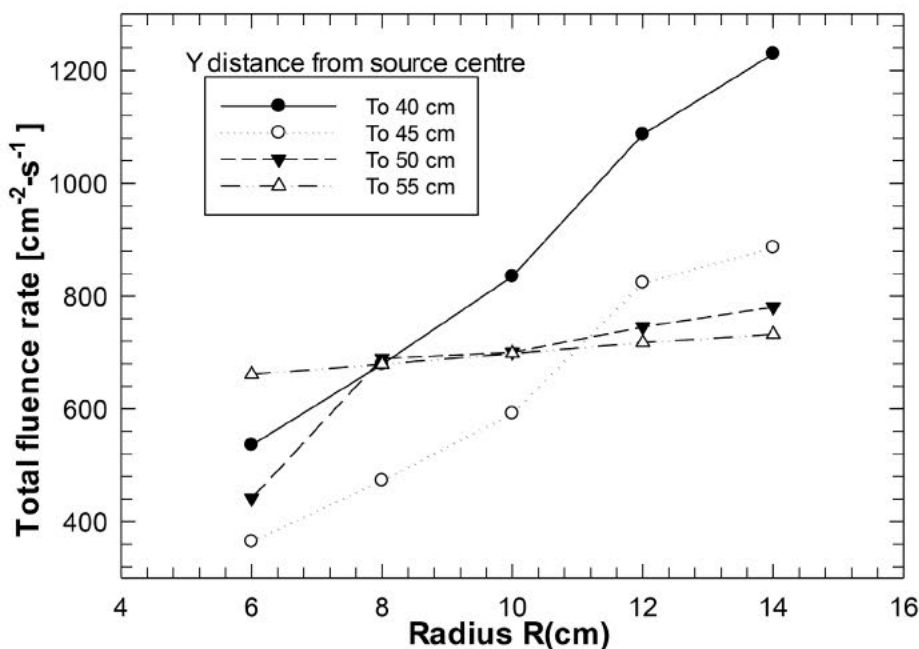


Fig. 6. Thermal neutron ($E < 0.4$ eV) fluence rate along radius points ($Z = 6; 8; 10; 12$ and 14 cm) at $X = 0$ and $Y = 40; 45; 50; 55$ cm from the source, with HDPE moderator.

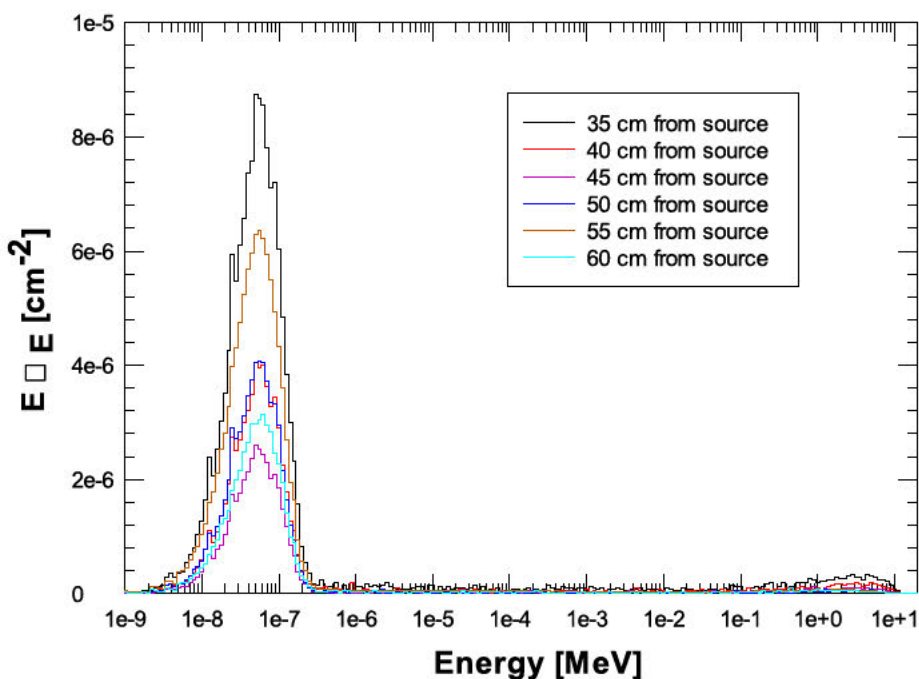


Fig. 7. Energy distribution of neutron fluence along the main axis of the irradiation chamber at points $X = 0; Z = 0$ and $Y = 35, 40; 45; 50; \text{ and } 60$ cm, with HDPE moderator.

flux, for a same geometry in graphite the total ambient dose equivalent would be almost double, due to leakage of neutrons from the device. Graphite produces fewer gamma radiation than HDPE, but it would need thicker layers compared to HDPE to reduce the neutron leakage contribution, due to its lower scattering cross section and smaller average energy loss per collision (Lacoste et al., 2004). This would be its main disadvantage.

Water and HDPE give lethargy spectra quite similar, see Fig. 5, and very close values of the thermal neutron flux ($9.11E+02 \pm 0.91 \text{ cm}^{-2} \text{ s}^{-1}$ and $9.04E+02 \pm 0.9 \text{ cm}^{-2} \text{ s}^{-1}$ respectively for $E < 0.4 \text{ eV}$). For a similar device (Bedogni et al., 2017) indicates the thermal fluence rate values from about $700 \text{ cm}^{-2} \text{ s}^{-1}$ to $1000 \text{ cm}^{-2} \text{ s}^{-1}$ moderated in HDPE at 50 cm from the $^{241}\text{Am}/^9\text{Be}$ source; these values are in agreement with the results obtained in this work of $9.04E+02 \pm 0.9 \text{ cm}^{-2} \text{ s}^{-1}$, at 40 cm from the $^{241}\text{Am}/^9\text{Be}$ source.

The objective of this work was to design a moderator device producing the maximum thermal neutron flux from an isotopic neutron source, allowing this device to reach the required thermal neutron fluxes that could be used hereafter in detection of trace materials through PGNA methods. In conclusion, the design made of HDPE is able to increase the thermal neutrons flux from the $^{241}\text{Am}/^9\text{Be}$ source, keeping the total ambient dose equivalent lower in comparison with water and graphite. The results displayed in Figs. 6 and 7 give useful information about the most appropriate points to place samples being analysed, where the low energy neutron flux is higher.

Acknowledgments

The first author Lenin E. Cevallos Robalino, thanks to *Secretaría de Educación Superior, Ciencia, Tecnología e Innovación of Ecuador* (SENESCYT), for the scholarship to carry out postgraduate studies in Madrid, Spain.

The author Gonzalo F. García Fernandez has developed this research work as part of Industrial Doctorate Program, IND2017/AMB 7797, funded by the Community of Madrid (CM), under the agreement between the Universidad Politécnica de Madrid (UPM) and the company *Biología y Técnica de la Radiación, S.L.* (Bioterra, S.L.).

References

Bedogni, R., Sacco, D., Gómez-Ros, J.M., Lorenzoli, M., Gentile, A., Buonomo, B., Pola, A., Introini, M.V., Bortot, D., Domingo, C., 2016. ETHERNES: a new design of radio-nuclide source-based thermal neutron facility with large homogeneity area. *Appl. Radiat. Isot.* 107, 171–176.

Bedogni, R., Sperduti, A., Pietropaolo, A., Pillon, M., Pola, A., Gómez-Ros, J.M., 2017. Experimental characterization of HOTNES: a new thermal neutron facility with large homogeneity area. *Nucl. Instrum. Methods Phys. Res.* 843, 18–21.

Belushkin, A., 1999. Neutron Scattering: History, Present State and Perspectives. vol. 152. Joint Institute for Nuclear Research, Dubna, pp. 30–46 E14.

Bom, V., Osman, A., Monem, A., 2008. A novel scanning land mine detector based on the

technique of neutron backscattering imaging. *IEEE Trans. Nucl. Sci.* 55, 741–747.

Chilton, A., Shultis, J., Faw, R., 1984. PRINCIPLES OF RADIATION SHIELDING, first ed. Prentice - Hill, New Jersey, USA.

Csikai, J., Dóczy, R., 2007. A comparison of the neutron thermalization and reflection methods used for bulk hydrogen analysis. *Appl. Radiat. Isot.* 65, 764–768.

Datema, C., Bom, V.R., Van-Eijk, C., 2002. DUNBLAD: the Delft University Neutron Backscattering Landmine Detector. 5th Monterrey Symposium on Technology and the Mine Problem, pp. 22–25 April 2002.

Douglas-Reilly, T., Ensslin, N., Smith, H., Kreiner, S., 1991. Passive Nondestructive Assay of Nuclear Materials. Report LA-UR-90-732. Los Alamos National Laboratory, USA.

El-Sayed Abdo, A., El-Sarraf, M., Gaber, F., 2003. Utilization of ilmenite/epoxy composite for neutrons and gamma rays attenuation. *Ann. Nucl. Energy* 30, 175–187.

Elsheikh, N., Viesti, G., El-Agib, I., Habbani, F., 2012. On the use of a ($^{252}\text{Cf}/^3\text{He}$) assembly for landmine detection by the neutron backscattering method. *Appl. Radiat. Isot.* 70, 643–649.

Gallego, E., Lorente, A., Vega-Carrillo, H.R., 2009. Testing of a high-density concrete as neutron shielding material. *Nucl. Technol.* 168–2, 399–404.

Glasstone, S., Sesonske, A., 1968. Ingeniería de reactores nucleares. España, Reverté, Primera edición, Barcelona.

Gokhale, P., Hussein, E., 1997. A ^{252}Cf neutron transmission technique for bulk detection of explosives. *Appl. Radiat. Isot.* 48, 973–979.

Hamidatou, L., Slamene, H., Akhal, T., Zouranen, B., 2013. Concepts, instrumentation and techniques of neutron activation analysis (Chapter 6). In: Kharfi, F. (Ed.), *Imaging and Radioanalytical Techniques in Interdisciplinary Research-Fundamentals and Cutting Edge Applications*. Intech, Rijeka, Croatia, pp. 141–178 published on.

Hassan, A., 2009. Bulk-samples Prompt Gamma-Rays Neutron Activation Analysis (PGNAA) with Isotopic Neutron Sources. Proceedings of the 7th Conference on Nuclear and Particle Physics. Sharm El-Sheikh, Egypt, pp. 69–78.

Hee-Jung, I., Song, K., 2009. Applications of prompt gamma ray neutron activation analysis: detection of illicit materials. *Appl. Spectrosc. Rev.* 44, 317–334.

ICRP, 1996. Conversion coefficients for use in radiological protection against external radiation. *Ann. ICRP* 26, 200 ICRP Report 74.

Lacoste, V., Gressier, V., Muller, H., Lebreton, L., 2004. Characterisation of the IRSN graphite moderated Americium-Beryllium neutron field. *Radiat. Protect. Dosim.* 110, 135–139.

Lee, H., Shin, H., Bae, S., 2012. A Polyethylene Moderator Design for Auxiliary Ex-Core Neutron Detector. Transactions of the Korean Nuclear Society Spring Meeting Jeju, Korea, pp. 17–18 May 2012.

Pelowitz, D., Fallgren, A., McMath, G., 2014. MCNP6TM User's Manual Code Version 6.1.1 Beta. Report LA-CP-14-0. Los Alamos National Laboratory, USA.

Soppera, N., Bossant, M., Dupont, E., 2014. JANIS 4: an improved version of the NEA java-based nuclear data information system. *Nucl. Data Sheets* 120, 294–296.

Travesi, A., 1975. ANÁLISIS POR ACTIVACIÓN NEUTRÓNICA. Ediciones JEN, Primera edición, Madrid, España.

Turhan, S., Yücel, H., Demirba, A., 2004. Prompt gamma neutron activation analysis of boron with a $^{241}\text{Am}/^9\text{Be}$ neutron source. *J. Radioanal. Nucl. Chem.* 262, 661–664.

Vega-Carrillo, H.R., Martínez-Ovalle, S.A., 2016. Few groups neutron spectra, and dosimetric, features, of isotopic neutron sources. *Appl. Radiat. Isot.* 117, 42–50.

Vega-Carrillo, H.R., Manzanares-Acuña, E., Hernández-Dávila, V.M., Gallego, E., Lorente, A., Donaire, I., 2007. Water-Extended Polyester neutron shield for a ^{252}Cf neutron source. *Radiat. Protect. Dosim.* 126, 269–273.

Vega-Carrillo, H.R., Gallego, E., Lorente, A., Rubio, I., 2009. Campo de neutrones en la sala de medidas neutrónicas de la Universidad Politécnica de Madrid. Report UaEN/RI-NEUT/UPM-03/05260609, España.

Vega-Carrillo, H.R., Benites-Rengifo, J.L., Hernandez-Davila, V.M., Ortiz-Rodriguez, J.M., De Leon-Martínez, H.A., 2016. NaI(Tl) Scintillator's response functions for point-like and distributed gamma-ray sources. *Journal of Nuclear Physics, Material Sciences, Radiation and Applications* 4, 129–137.

Vitorelli, J., Silva, A., Crispim, V., Da Fonseca, E., Pereira, W., 2005. Monte Carlo Simulation of response function for a NaI(Tl) detector for gamma rays from $^{241}\text{Am}/^9\text{Be}$ source. *Appl. Radiat. Isot.* 62, 619–622.

Yasin, T., Khan, M., 2008. High density polyethylene/boron carbide composites for neutron shielding. *E-Polymers* 59, 1–7.